PAPER Special Section on Selected Papers from the 20th Workshop on Circuits and Systems in Karuizawa

A Palmprint Recognition Algorithm Using Phase-Only Correlation

Koichi ITO[†a)], **Takafumi AOKI**[†], ***Members***, **Hiroshi NAKAJIMA**[††], ***Nonmember***, **Koji KOBAYASHI**[††], ***Member***, ***and*** **Tatsuo HIGUCHI**[†††], ***Fellow***

SUMMARY This paper presents a palmprint recognition algorithm using Phase-Only Correlation (POC). The use of phase components in 2D (two-dimensional) discrete Fourier transforms of palmprint images makes it possible to achieve highly robust image registration and matching. In the proposed algorithm, POC is used to align scaling, rotation and translation between two palmprint images, and evaluate similarity between them. Experimental evaluation using a palmprint image database clearly demonstrates efficient matching performance of the proposed algorithm.

key words: *biometrics, palmprint recognition, security, image recognition, phase-only correlation*

1. Introduction

With the increased demands in reliable personal identification, biometric authentication has been receiving much attention over the past decade [1]. Biometric authentication is to identify individuals using physiological or behavioral characteristics, such as fingerprint, face, iris, hand, gait, gesture, etc. Biometrics provides better security and greater convenience than the traditional authentication using passwords, keys and numbers, since passwords or numbers may be forgotten, and keys may be stolen or lost. Among many biometric techniques, palmprint recognition is one of the most reliable approaches, since a palm, the large inner surface of a hand, contains many features such as principle lines, ridges, minutiae points, singular points and texture [2].

Previous works on palmprint recognition employ the feature-based approach which is to extract feature vectors corresponding to individual palmprint images and perform palmprint matching based on some distance metrics [2]–[5]. In some papers, geometrical and structural features of principle lines [2], ridges and minutia points [3] are used for palmprint matching. The other papers employ Gabor filters to extract palmprint features [2], [4], [5]. One of the difficult problems in feature-based palmprint recognition is that the matching performance is significantly influenced by many parameters in feature extraction process, which may vary depending on environmental factors of palmprint image acquisition.

This paper presents an efficient algorithm for palmprint recognition using Phase-Only Correlation (POC) — an image matching technique using the phase components in 2D Discrete Fourier Transforms (DFTs) of given images. The technique has been successfully applied to sub-pixel image registration tasks for computer vision applications [6], [7]. In our previous works [8]–[10], we have proposed a fingerprint recognition algorithm using POC, which has already been implemented in actual fingerprint verification units [11]. We have also proposed an iris recognition algorithm using POC [12]. In this paper, we demonstrate that the POC technique is also highly effective for palmprint recognition. Experimental evaluation using the PolyU palmprint database [13] clearly demonstrates efficient matching performance of the proposed algorithm compared with a conventional feature-based algorithm.

This paper is organized as follows: Sect. 2 describes the fundamental definition of POC, the modified version of POC for biometric authentication, and the scaling and rotation estimation method using POC. Section 3 describes a palmprint recognition algorithm using POC. Section 4 presents a set of experiments for evaluating recognition performance of the proposed algorithm. In Sect. 5, we end with some conclusions.

2. Phase-Only Correlation

2.1 Fundamental Definition

We introduce the principle of the Phase-Only Correlation (POC) function (which is sometimes called the "phase-correlation function") [6], [7], [14].

Consider two $N_1 \times N_2$ images, $f(n_1, n_2)$ and $g(n_1, n_2)$, where we assume that the index ranges are $n_1 = -M_1, \cdots, M_1$ ($M_1 > 0$) and $n_2 = -M_2, \cdots, M_2$ ($M_2 > 0$), and hence $N_1 = 2M_1 + 1$ and $N_2 = 2M_2 + 1$. Note that we assume here the sign symmetric index ranges $\{-M_1, \cdots, M_1\}$ and $\{-M_2, \cdots, M_2\}$ for mathematical simplicity. The discussion could be easily generalized to non-negative index ranges with power-of-two image size. Let $F(k_1, k_2)$ and $G(k_1, k_2)$ denote the 2D DFTs of the two images, which are given by

Manuscript received July 1, 2007.
Manuscript revised October 5, 2007.

[†]The authors are with the Department of Computer and Mathematical Sciences, Graduate School of Information Sciences, Tohoku University, Sendai-shi, 980-8579 Japan.
[††]The authors are with Yamatake Corporation, Fujisawa-shi, 251-8522 Japan.
[†††]The author is with the Faculty of Engineering, Tohoku Institute of Technology, Sendai-shi, 982-8577 Japan.
a) E-mail: ito@aoki.ecei.tohoku.ac.jp

DOI: 10.1093/ietfec/e91–a.4.1023

$$F(k_1,k_2) = \sum_{n_1,n_2} f(n_1,n_2) W_{N_1}^{k_1 n_1} W_{N_2}^{k_2 n_2} = A_F(k_1,k_2) e^{j\theta_F(k_1,k_2)}, \quad (1)$$

$$G(k_1,k_2) = \sum_{n_1,n_2} g(n_1,n_2) W_{N_1}^{k_1 n_1} W_{N_2}^{k_2 n_2} = A_G(k_1,k_2) e^{j\theta_G(k_1,k_2)}, \quad (2)$$

where $k_1 = -M_1, \cdots, M_1$, $k_2 = -M_2, \cdots, M_2$, $W_{N_1} = e^{-j\frac{2\pi}{N_1}}$, $W_{N_2} = e^{-j\frac{2\pi}{N_2}}$, and $\sum_{n_1,n_2}$ denotes $\sum_{n_1=-M_1}^{M_1} \sum_{n_2=-M_2}^{M_2}$. $A_F(k_1,k_2)$ and $A_G(k_1,k_2)$ are amplitude components, and $\theta_F(k_1,k_2)$ and $\theta_G(k_1,k_2)$ are phase components. The cross-phase spectrum $R_{FG}(k_1,k_2)$ is given by

$$R_{FG}(k_1,k_2) = \frac{F(k_1,k_2)\overline{G(k_1,k_2)}}{|F(k_1,k_2)\overline{G(k_1,k_2)}|} = e^{j\theta(k_1,k_2)}, \quad (3)$$

where $\overline{G(k_1,k_2)}$ is the complex conjugate of $G(k_1,k_2)$ and $\theta(k_1,k_2)$ denotes the phase difference $\theta_F(k_1,k_2) - \theta_G(k_1,k_2)$. The POC function $r_{fg}(n_1,n_2)$ is the 2D Inverse DFT (2D IDFT) of $R_{FG}(k_1,k_2)$ and is given by

$$r_{fg}(n_1,n_2) = \frac{1}{N_1 N_2} \sum_{k_1,k_2} R_{FG}(k_1,k_2) \times W_{N_1}^{-k_1 n_1} W_{N_2}^{-k_2 n_2}, \quad (4)$$

where $\sum_{k_1,k_2}$ denotes $\sum_{k_1=-M_1}^{M_1} \sum_{k_2=-M_2}^{M_2}$. When two images are similar, their POC function gives a distinct sharp peak. When two images are not similar, the peak drops significantly. The height of the peak gives a good similarity measure for image matching, and the location of the peak shows the translational displacement between the images. Other important properties of POC used for biometric authentication tasks is that it is not influenced by image shift and brightness change, and it is highly robust against noise. See [8] for detailed discussions.

2.2 Band-Limited Phase-Only Correlation (BLPOC)

We have proposed the idea of BLPOC (Band-Limited Phase-Only Correlation) function for efficient matching of fingerprint images considering the inherent frequency components of their images [8]. Through a set of experiments, we have found that the same idea is also very effective for palmprint images. The idea of the BLPOC function is to eliminate meaningless high frequency components in the calculation of cross-phase spectrum $R_{FG}(n_1,n_2)$ depending on the inherent frequency components of palmprint images. The original POC function $r_{fg}(n_1,n_2)$ emphasizes the high frequency components, which may have less reliability. We observe that this reduces the height of the correlation peak significantly even if the given two images are captured from the same person. On the other hand, the BLPOC function allows us to evaluate the similarity using the inherent frequency band within palmprint textures.

Assume that the ranges of the inherent frequency band are given by $k_1 = -K_1, \cdots, K_1$ and $k_2 = -K_2, \cdots, K_2$, where $0 \le K_1 \le M_1$ and $0 \le K_2 \le M_2$. Thus, the effective size of frequency spectrum is given by $L_1 = 2K_1 + 1$ and $L_2 = 2K_2 + 1$. The BLPOC function is given by

$$r_{fg}^{K_1 K_2}(n_1,n_2) = \frac{1}{L_1 L_2} \sum_{k_1,k_2}{}' R_{FG}(k_1,k_2) \times W_{L_1}^{-k_1 n_1} W_{L_2}^{-k_2 n_2}, \quad (5)$$

where $n_1 = -K_1, \cdots, K_1$, $n_2 = -K_2, \cdots, K_2$, and $\sum'_{k_1,k_2}$ denotes $\sum_{k_1=-K_1}^{K_1} \sum_{k_2=-K_2}^{K_2}$. Note that the maximum value of the correlation peak of the BLPOC function is always normalized to 1 and does not depend on L_1 and L_2.

The peak location of the BLPOC function also indicates the translational displacement between two images as well as that of the POC function. Note, however, that in the case of the BLPOC function, we have to convert the peak location into the displacement according to the following procedure, since the peak location of the BLPOC function does not directly denote the displacement between two images. We first estimate the true peak position $(\tilde{\delta}_1, \tilde{\delta}_2)$ of the BLPOC function using the function fitting technique [7] or PEF (Peak Evaluation Formula) [15] based on the closed-form peak model of the POC function. Then, we normalize $(\tilde{\delta}_1, \tilde{\delta}_2)$ according to the parameters K_1/M_1 and K_2/M_2 to obtain the sub-pixel displacement (δ_1, δ_2) as follows

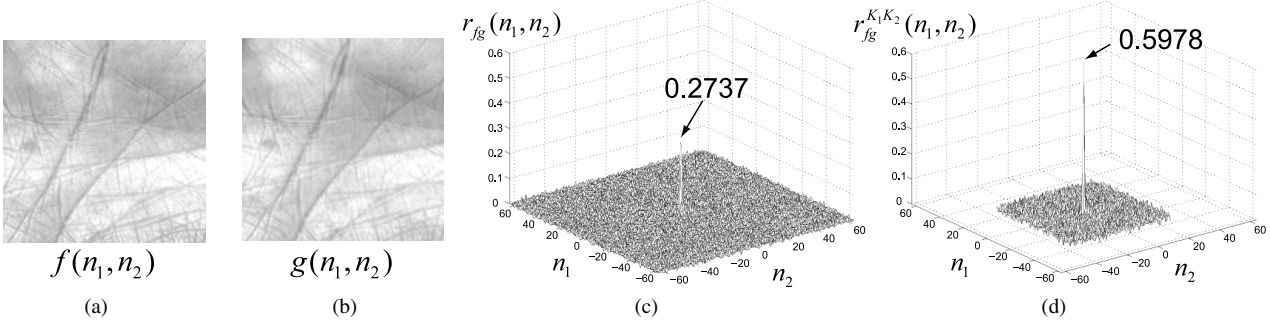

Fig. 1 Example of genuine matching using the original POC function and the BLPOC function: (a) Input palmprint image $f(n_1,n_2)$, (b) registered palmprint image $g(n_1,n_2)$, (c) original POC function $r_{fg}(n_1,n_2)$ and (d) BLPOC function $r_{fg}^{K_1K_2}(n_1,n_2)$ with $K_1/M_1 = 0.5$ and $K_2/M_2 = 0.5$.

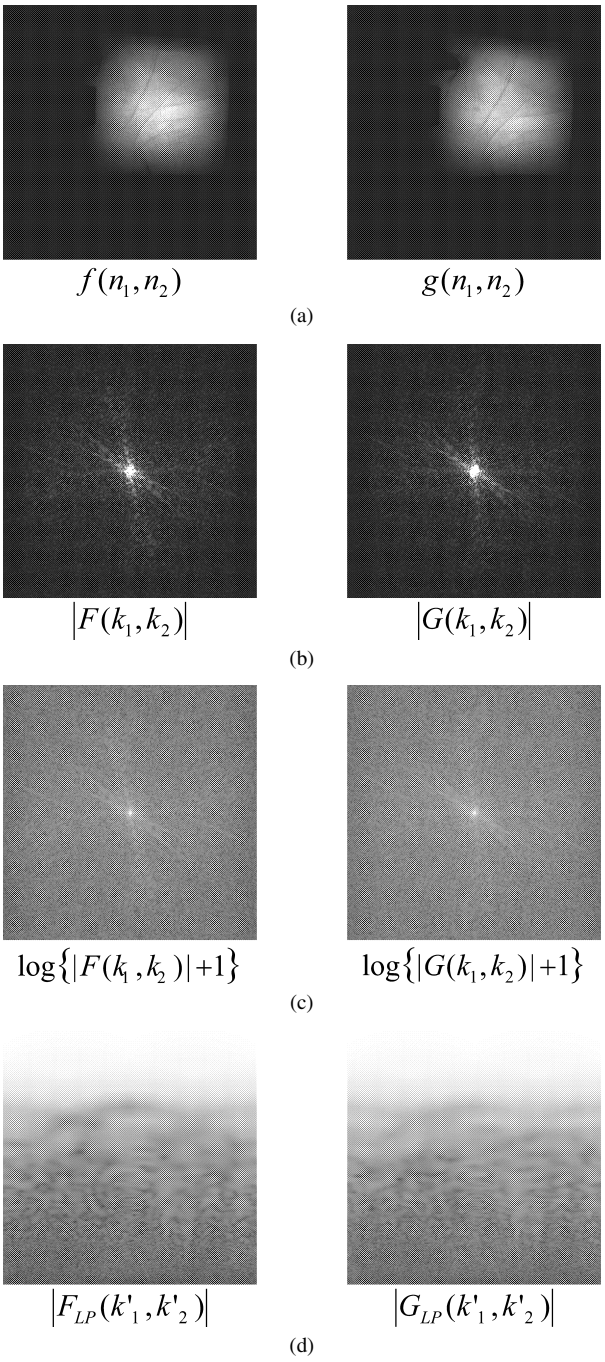

Fig. 2 Scaling and rotation estimation using POC: (a) The input image and the registered image, (b) the amplitude spectra of images, (c) enhanced amplitude spectra and (d) log-polar mappings of the amplitude spectra.

$$\delta_1 = \tilde{\delta}_1 \times \frac{2M_1 + 1}{2K_1 + 1}, \quad \delta_2 = \tilde{\delta}_2 \times \frac{2M_2 + 1}{2K_2 + 1}. \tag{6}$$

Our observation shows that the accuracy of displacement estimation using the BLPOC function is comparable with that of using the POC function. In this paper, we employ the BLPOC function to estimate the translational displacement between images.

Figure 1 shows an example of genuine matching using the original POC function $r_{fg}(n_1, n_2)$ and the BLPOC function $r_{fg}^{K_1 K_2}(n_1, n_2)$. The BLPOC function provides the higher correlation peak and better discrimination capability than that of the original POC function.

2.3 Scale Factor and Rotation Angle Estimation Using POC

The translation estimation method using POC can be extended to the registration for images including translation, rotation and scaling simultaneously [7]. We employ the log-polar mapping of the amplitude spectrum to transform the image scaling and rotation into image translation. The scale factor and rotation angle are estimated by detecting the corresponding translational displacements using POC. We summarize the procedure for estimating the scale factor κ and the rotation angle θ between images $f(n_1, n_2)$ and $g(n_1, n_2)$ as follows (see [7] for detailed discussions).

1. Calculate 2D DFTs of $f(n_1, n_2)$ and $g(n_1, n_2)$ to obtain $F(k_1, k_2)$ and $G(k_1, k_2)$.
2. Calculate amplitude spectra $|F(k_1, k_2)|$ and $|G(k_1, k_2)|$ and treat them as real-valued images (Fig. 2(b)). For natural images, most energy is concentrated in low-frequency domain. Hence, we had better to use $\log\{|F(k_1, k_2)| + 1\}$ and $\log\{|G(k_1, k_2)| + 1\}$ (or $\sqrt{|F(k_1, k_2)|}$ and $\sqrt{|G(k_1, k_2)|}$) instead of $|F(k_1, k_2)|$ and $|G(k_1, k_2)|$ (Fig. 2(c)).
3. Calculate the log-polar mappings $|F_{LP}(k'_1, k'_2)|$ and $|G_{LP}(k'_1, k'_2)|$ (Fig. 2(d)).
4. Estimate the image displacement between $|F_{LP}(k'_1, k'_2)|$ and $|G_{LP}(k'_1, k'_2)|$ using the peak location of the BLPOC function $r_{|F_{LP}||G_{LP}|}^{K_1 K_2}(n_1, n_2)$ to obtain κ and θ.

3. Palmprint Recognition Algorithm

In this section, we present a palmprint recognition algorithm using POC. The proposed algorithm consists of four steps: (i) scaling and rotation alignment, (ii) translation alignment, (iii) effective region extraction and (iv) matching score calculation (Fig. 3).

Step 1: Scaling and rotation alignment

We need to normalize scaling, rotation and translation between the input image $f(n_1, n_2)$ and the registered image $g(n_1, n_2)$ in order to perform the high-accuracy palmprint matching.

At first, we reduce the effect of background components in palmprint images by applying 2D spatial window to the two images $f(n_1, n_2)$ and $g(n_1, n_2)$. The 2D spatial window is applied at the center of gravity of each palmprint to align scaling, rotation and translation between the two images $f(n_1, n_2)$ and $g(n_1, n_2)$ correctly. In this paper, we use 2D Hanning window as 2D spatial window. The center of gravity (c_1, c_2) of each palmprint is detected as follows (Fig. 5): (i) compute n_2-axis projection $p_{n_2}(n_1)$ and n_1-axis projection $p_{n_1}(n_2)$ of pixel values as

procedure *Palmprint recognition using POC*
Input
$f(n_1, n_2)$: the palmprint image to be identified,
$g(n_1, n_2)$: the registered palmprint image;
Output
the matching score between $f(n_1, n_2)$ and $g(n_1, n_2)$;

1. **begin**
2. detect the center of gravity of each palmprint using pixel-value projection;
3. apply 2D spatial window to the two images $f(n_1, n_2)$ and $g(n_1, n_2)$ at the center of gravity of each palmprint to obtain $f_w(n_1, n_2)$ and $g_w(n_1, n_2)$;
4. estimate the scale factor κ and the rotation angle θ between $f_w(n_1, n_2)$ and $g_w(n_1, n_2)$ using the method described in Sect. 2.3 and obtain the scale- and rotation-normalized image $g_{w\kappa\theta}(n_1, n_2)$;
5. estimate the translational displacement (δ_1, δ_2) between $f_w(n_1, n_2)$ and $g_{w\kappa\theta}(n_1, n_2)$ using BLPOC and obtain the normalized images $f'(n_1, n_2)$ and $g'(n_1, n_2)$;
6. extract the effective palmprint regions $f''(n_1, n_2)$ and $g''(n_1, n_2)$ from $f'(n_1, n_2)$ and $g'(n_1, n_2)$ using pixel-value projection;
7. calculate the BLPOC function $r^{K_1 K_2}_{f''g''}(n_1, n_2)$;
8. compute the sum of the highest P peaks of $r^{K_1 K_2}_{f''g''}(n_1, n_2)$ as the matching score
9. **end.**

Fig. 3 Palmprint recognition algorithm using POC.

$$p_{n_2}(n_1) = \sum_{n_2=-M_2}^{M_2} f(n_1, n_2)/N_2, \tag{7}$$

$$p_{n_1}(n_2) = \sum_{n_1=-M_1}^{M_1} f(n_1, n_2)/N_1, \tag{8}$$

(ii) compute the mean values $\mu_{p_{n_2}}$ and $\mu_{p_{n_1}}$ for the two projections $p_{n_2}(n_1)$ and $p_{n_1}(n_2)$, respectively, and (iii) define the center of gravity (c_1, c_2) as

$$c_1 = \{\max(\{n_1 | p_{n_2}(n_1) \geq \mu_{p_{n_2}}, -M_1 \leq n_1 \leq M_1\}) + \min(\{n_1 | p_{n_2}(n_1) \geq \mu_{p_{n_2}}, -M_1 \leq n_1 \leq M_1\})\}/2, \tag{9}$$

$$c_2 = \{\max(\{n_2 | p_{n_1}(n_2) \geq \mu_{p_{n_1}}, -M_2 \leq n_2 \leq M_2\}) + \min(\{n_2 | p_{n_1}(n_2) \geq \mu_{p_{n_1}}, -M_2 \leq n_2 \leq M_2\})\}/2. \tag{10}$$

Figure 4(a) shows the palmprint images and their centers of gravity, and (b) shows the palmprint images, $f_w(n_1, n_2)$ and $g_w(n_1, n_2)$, after applying 2D Hanning window.

Next, we estimate the scale factor κ and the rotation angle θ using the technique described in Sect. 2.3. Using κ and θ, we obtain a scaling- and rotation-normalized image $g_{w\kappa\theta}(n_1, n_2)$.

Step 2: Translation alignment

Then, we align the translational displacement between $f_w(n_1, n_2)$ and $g_{w\kappa\theta}(n_1, n_2)$ using the technique described in Sect. 2.2. Thus, we have normalized versions of the input image and the registered image as shown in Fig. 4(c), which are denoted by $f'(n_1, n_2)$ and $g'(n_1, n_2)$.

Step 3: Effective region extraction

This step is to extract the effective region of the two images $f'(n_1, n_2)$ and $g'(n_1, n_2)$. This process improves the accuracy of palmprint matching, since the non-overlapped areas of the two images become the uncorrelated noise components in the BLPOC function. The effective palmprint ar-

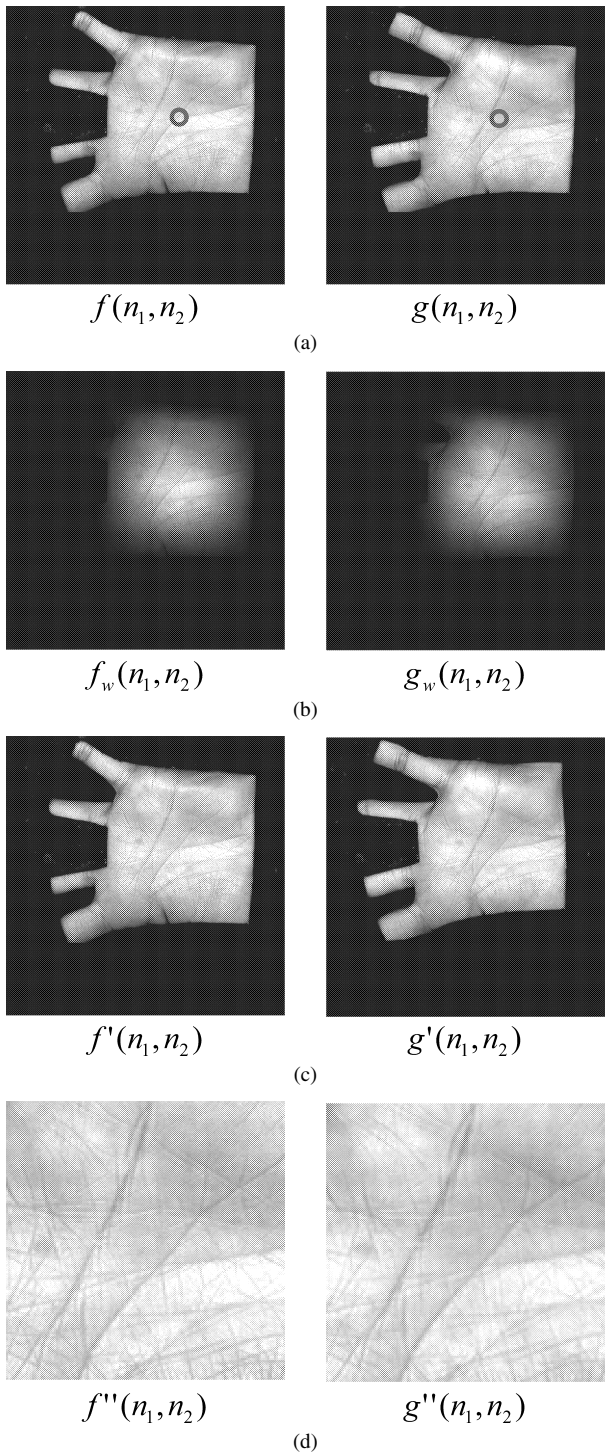

Fig. 4 Scaling, rotation and displacement alignment and effective region extraction: (a) The input image $f(n_1, n_2)$, the registered image $g(n_1, n_2)$, and their centers of gravity, (b) images, $f_w(n_1, n_2)$ and $g_w(n_1, n_2)$, after applying 2D Hanning window, (c) normalized images $f'(n_1, n_2)$ and $g'(n_1, n_2)$, and (d) extracted effective regions $f''(n_1, n_2)$ and $g''(n_1, n_2)$.

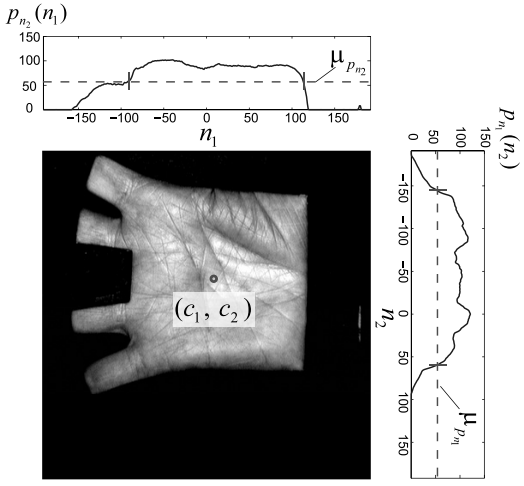

Fig. 5 Center of gravity detection using pixel-value projection.

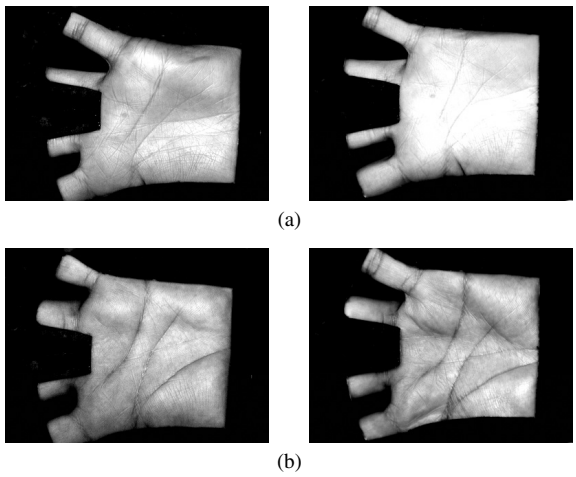

Fig. 6 Examples of palmprint images in the PolyU palmprint database: palmprint image pairs with different lighting condition (a) and nonlinear distortion (b).

eas in the input image $f'(n_1, n_2)$ and the registered image $g'(n_1, n_2)$ are extracted as follows: (i) detect the centers of gravity, $(c_1^{f'}, c_2^{f'})$ and $(c_1^{g'}, c_2^{g'})$, of two images using the procedure described in Step 1, (ii) compute the mean values of the two centers of gravity as

$$\bar{c}_1 = (c_1^{f'} + c_1^{g'})/2, \quad \bar{c}_2 = (c_2^{f'} + c_1^{g'})/2, \tag{11}$$

(iii) extract $m_1 \times m_2$ regions centered on $(\bar{c}_1, \bar{c}_2)$ from $f'(n_1, n_2)$ and $g'(n_1, n_2)$. Through the above procedure, only the common effective image areas, $f''(n_1, n_2)$ and $g''(n_1, n_2)$, with the same size ($m_1 \times m_2$ pixels) are extracted for the succeeding image matching step (Fig. 4(d)).

Step 4: Matching score calculation

We calculate the BLPOC function $r_{f''g''}^{K_1 K_2}(n_1, n_2)$ between the two extracted images $f''(n_1, n_2)$ and $g''(n_1, n_2)$, and compute the matching score. The matching score is the sum of the highest P peaks of the BLPOC function $r_{f''g''}^{K_1 K_2}(n_1, n_2)$.

4. Experiments and Discussions

This section describes a set of experiments using the PolyU palmprint database [13] for evaluating palmprint recognition performance of the proposed algorithm. This database consists of 600 images (384 × 284 pixels) with 100 subjects and 6 different images of each palmprint. Note that both even and odd pixels are acceptable image sizes for the proposed algorithm. Figure 6 shows some examples of palmprint images in this database. As shown in this figure, palmprint images in the database are captured under different lighting condition and have nonlinear distortion due to movement of fingers.

The performance of the biometrics-based verification system is evaluated by the Receiver Operating Characteristic (ROC) curve, which illustrates the False Rejection Rate (FRR) against the False Acceptance Rate (FAR) at different thresholds on the matching score. We first evaluate the FRR for all the possible combinations of genuine attempts; the number of attempts is ${}_6C_2 \times 100 = 1,500$. Next, we evaluate the FAR for ${}_{100}C_2 = 4,950$ impostor attempts, where we select a single image (the first image) for each palmprint and make all the possible combinations of impostor attempts. The performance is also evaluated by the Equal Error Rate (EER), which is defined as the error rate where the FAR and the FRR are equal.

In the followings, we describe experiments for (i) performance optimization of the proposed algorithm and (ii) performance comparison with the conventional palmprint recognition algorithm.

4.1 Performance Optimization

We consider reducing the computation time while optimizing the matching performance of the proposed algorithm by changing the palmprint image size, the bandwidth parameters of BLPOC function K_1/M_1 and K_2/M_2, and the number of peaks P for the matching score calculation, respectively. In our previous work on phase-based fingerprint recognition [10], we can reduce the image size without considerable degradation of matching performance. We expect that the similar tendency is observed in the phase-based palmprint recognition. In this experiment, the image reduction ratio for palmprint images is changed from 10% to 100%, the parameters K_1/M_1 and K_2/M_2 are changed from 0.05 to 1.00 and the parameter P is changed from 1 to 9. The size of effective region is set to $m_1 = m_2 = 128$ when the reduction ratio is 100 %. In other cases, m_1 and m_2 are changed depending on the reduction ratio. The computation time is evaluated by using MATLAB 6.5.1 on Pentium4 3.2 GHz.

Table 1 shows the reduction ratio, EER, the parameters K_1/M_1 and K_2/M_2, and the number of peaks P, where K_1/M_1, K_2/M_2 and P are optimized for every reduction ratio. Figure 7 plots EER and computation time against the reduction ratio. As a result, the optimal matching performance is observed when the image reduction ratio is 50%,

Table 1 Experimental results of performance optimization.

Reduction ratio [%]	EER [%]	K_1/M_1 and K_2/M_2	P
10	6.64	0.85	2
15	1.86	0.90	4
20	0.53	0.80	4
25	0.46	0.65	3
30	0.24	0.65	2
35	0.37	0.75	3
40	0.23	0.50	7
45	0.17	0.75	4
50	0.12	0.75	1
55	0.24	0.85	2
60	0.16	0.70	2
65	0.31	0.30	5
70	0.37	0.25	6
75	0.50	0.64	2
80	0.44	0.20	5
85	0.44	0.55	1
90	0.50	0.15	4
95	0.51	0.30	6
100	0.46	0.25	4

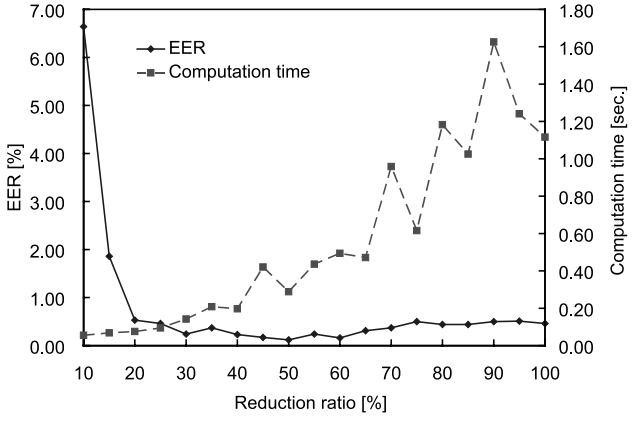

Fig. 7 EER and computation time against the image size reduction.

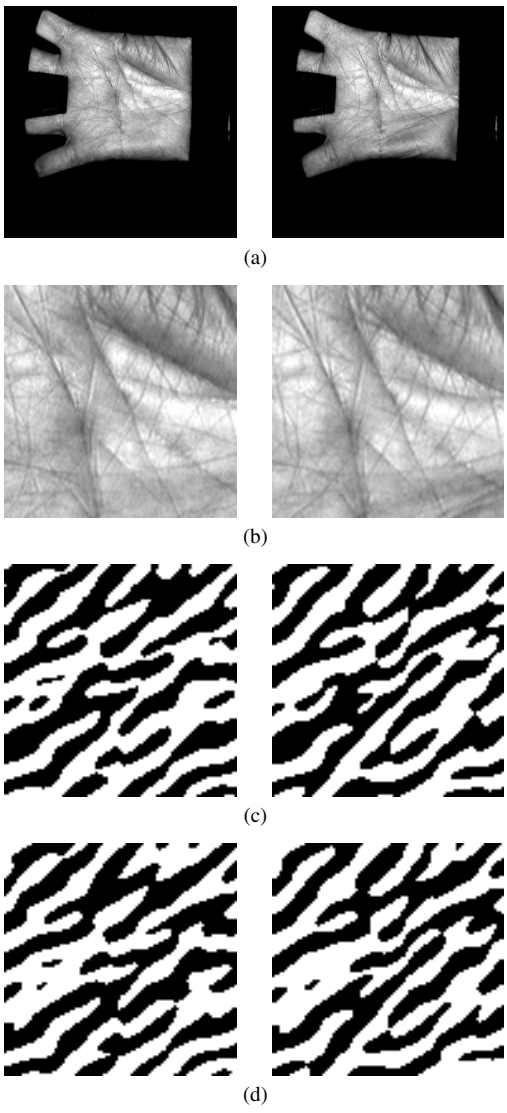

Fig. 8 Palmprint features obtained by 2D Gabor filtering: (a) Input and registered images, (b) extracted effective regions, (c) and (d) real part and imaginary part of extracted palmprint features, respectively.

$K_1/M_1 = K_2/M_2 = 0.75$ and $P = 1$. In this case, the EER of the proposed algorithm is 0.12% and the computation time is 0.29 seconds. The optimal parameters K_1/M_1 and K_2/M_2 are higher than those for other biometric recognition using POC. For example, the parameters of BLPOC function are $K_1/M_1 = K_2/M_2 = 0.40$ for fingerprint recognition [8], $K_1/M_1 = 0.6$ and $K_2/M_2 = 0.2$ for iris recognition [12], respectively. This fact indicates that the important information of the palmprint images in the frequency domain spreads to a wide range of frequencies compared with fingerprint images and iris images. Thus, we need to design the BLPOC function depending on each biometric modalities in order to achieve accurate recognition.

4.2 Performance Comparison with the Conventional Algorithm

We compare two different matching algorithms: (A) a conventional palmprint recognition algorithm [4] and (B) the proposed algorithm.

The conventional algorithm used in this paper is summarized as follows: (i) align two palmprint images, (ii) extract effective regions of palmprint images (Fig. 8(b)), (iii) extract palmprint feature vectors using the 2D Gabor phase coding scheme which has been used for iris recognition [16] (Figs. 8(c) and (d)), (iv) compute a normalized Hamming distance, i.e., dissimilarity, between two palmprint feature vectors. In the steps (i) and (ii), we employ the same processes used in the proposed algorithm, where the size of effective region is 128×128 pixels. In the step (iii), we employ the same parameter set of 2D Gabor filter used in [4].

Figure 9 shows the ROC curves for the two algorithms. The proposed algorithm (B) exhibits significantly higher performance, since its ROC curve is located at lower FRR/FAR region than that of the conventional algorithm (A). The EER of the proposed algorithm (B) is 0.12%, while the EER of the conventional algorithm (A) is 0.45%. The computation time of the proposed algorithm is 0.29 seconds,

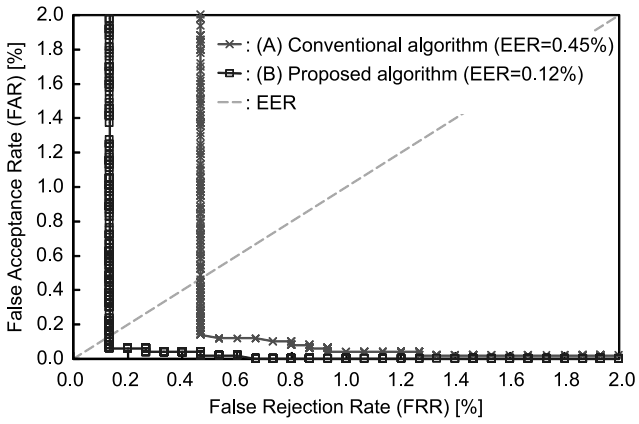

Fig. 9 ROC curves and EERs.

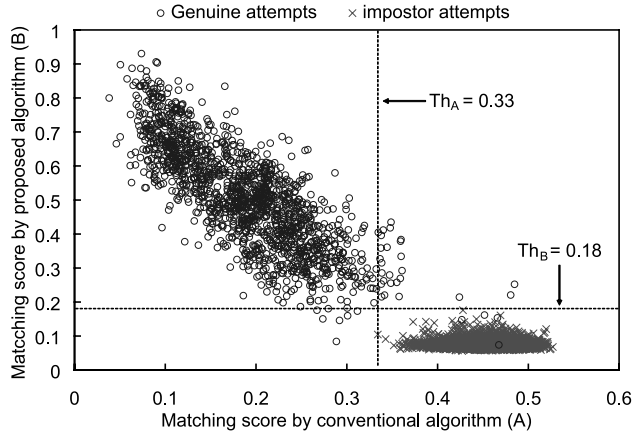

Fig. 10 Overall joint distribution of matching scores for the proposed algorithm and the conventional algorithm.

while that of the conventional algorithm is 1.37 seconds.

Figure 10 shows the joint distribution of matching scores for the two algorithms (A) and (B). The vertical dashed line indicates the highest impostor's score of the conventional algorithm (A) and the horizontal dashed line indicates the highest impostor's score of the proposed algorithm (B). In practical biometric verification system, the highest impostor's score Th_A (or Th_B) is used as the threshold value of verification in order to guarantee the condition FAR = 0. Under this condition, the conventional algorithm (A) accepts only 98.00% of genuine palmprints and rejects the remaining 2.00%, while the proposed algorithm (B) accepts 99.33% of genuine palmprints and rejects only 0.67% of them.

As is observed in the above experiments, the proposed algorithm is particularly useful for verifying palmprint images.

5. Conclusion

This paper proposed a palmprint recognition algorithm using the Phase-Only Correlation (POC). The use of POC makes it possible to align palmprint images and evaluate similarity between them correctly. Experimental performance evaluation demonstrates efficient performance of our proposed algorithm compared with the conventional palmprint recognition algorithm.

We expect that a compact system configuration will be available to implement the palmprint recognition system based on the proposed algorithm. Our preliminary observation shows that palmprint images taken with a cell phone camera, e.g., the image size is 352×288 pixels, are enough for the proposed algorithm to achieve reliable palmprint recognition. Also, the DSP (Digital Signal Processor) can be used to achieve real-time recognition capability as well as the iris recognition system [17]. Thus, we will implement a compact and low-cost palmprint recognition system using the proposed algorithm.

We have already demonstrated that the POC-based image matching is also effective for fingerprint and iris recognition tasks. Hence, we can expect that the proposed approach may be useful for mulitimodal biometric system having palmprint, fingerprint and iris recognition capabilities.

Acknowledgment

Portions of the research in this paper use the PolyU palmprint database collected by Hong Kong Polytechnic University.

References

[1] A. Jain, A. Ross, and S. Prabhakar, "An introduction to biometric recognition," IEEE Trans. Circuits Syst. Video Technol., vol.14, no.1, pp.4–20, Jan. 2004.
[2] D. Zhang, Palmprint Authentication, Kluwer Academic Publication, 2004.
[3] N. Duta, A. Jain, and K. Mardia, "Matching of palmprints," Pattern Recognition Letters, vol.23, no.4, pp.477–485, 2002.
[4] D. Zhang, W.K. Kong, J. You, and M. Wong, "Online palmprint identification," IEEE Trans. Pattern Anal. Mach. Intell., vol.25, no.9, pp.1041–1050, Sept. 2003.
[5] A. Kong, D. Zhang, and M. Kamel, "Palmprint identification using feature-level fusion," Pattern Recognit., vol.39, pp.478–487, 2006.
[6] C.D. Kuglin and D.C. Hines, "The phase correlation image alignment method," Proc. Int. Conf. Cybernetics and Society, pp.163–165, 1975.
[7] K. Takita, T. Aoki, Y. Sasaki, T. Higuchi, and K. Kobayashi, "High-accuracy subpixel image registration based on phase-only correlation," IEICE Trans. Fundamentals, vol.E86-A, no.8, pp.1925–1934, Aug. 2003.
[8] K. Ito, H. Nakajima, K. Kobayashi, T. Aoki, and T. Higuchi, "A fingerprint matching algorithm using phase-only correlation," IEICE Trans. Fundamentals, vol.E87-A, no.3, pp.682–691, March 2004.
[9] K. Ito, A. Morita, T. Aoki, T. Higuchi, H. Nakajima, and K. Kobayashi, "A fingerprint recognition algorithm combining phase-based image matching and feature-based matching," Lect. Notes Comput. Sci. (ICB2006), vol.3832, pp.316–325, Dec. 2005.
[10] H. Nakajima, K. Kobayashi, M. Morikawa, A. Katsumata, K. Ito, T. Aoki, and T. Higuchi, "Fast and robust fingerprint identification algorithm and its application to residential access control products," Lect. Notes Comput. Sci. (ICB2006), vol.3832, pp.326–333, Dec. 2005.
[11] Products using phase-based image matching, http://www.aoki.ecei.tohoku.ac.jp/research/poc.html

[12] K. Miyazawa, K. Ito, T. Aoki, K. Kobayashi, and H. Nakajima, "A phase-based iris recognition algorithm," Lect. Notes Comput. Sci. (ICB2006), vol.3832, pp.356–365, Dec. 2005.
[13] PolyU Palmprint Database, http://www4.comp.polyu.edu.hk/~biometrics/
[14] K. Takita, M.A. Muquit, T. Aoki, and T. Higuchi, "A sub-pixel correspondence search technique for computer vision applications," IEICE Trans. Fundamentals, vol.E87-A, no.8, pp.1913–1923, Aug. 2004.
[15] S. Nagashima, T. Aoki, T. Higuchi, and K. Kobayashi, "A sub-pixel image matching technique using phase-only correlation," Proc. IEEE 2006 Int. Symp. Intelligent Signal Processing and Communication Systems, pp.701–704, Dec. 2006.
[16] J. Daugman, "High confidence visual recognition of persons by a test of statistical independence," IEEE Trans. Pattern Anal. Mach. Intell., vol.15, no.11, pp.1148–1161, Nov. 1993.
[17] K. Miyazawa, K. Ito, T. Aoki, K. Kobayashi, and A. Katsumata, "An iris recognition system using phase-based image matching," Proc. 2006 IEEE Int. Conf. Image Processing, pp.325–328, Oct. 2006.

Koichi Ito received the B.E. degree in electronic engineering, and the M.S. and Ph.D. degree in information sciences from Tohoku University, Sendai, Japan, in 2000, 2002 and 2005, respectively. He is currently an Assistant Professor of the Graduate School of Information Sciences at Tohoku University. From 2004 to 2005, he was a Research Fellow of the Japan Society for the Promotion of Science. His research interests include signal and image processing, and biometric authentication.

Takafumi Aoki received the B.E., M.E., and D.E. degrees in electronic engineering from Tohoku University, Sendai, Japan, in 1988, 1990, and 1992, respectively. He is currently a Professor of the Graduate School of Information Sciences at Tohoku University. For 1997–1999, he also joined the PRESTO project, Japan Science and Technology Corporation (JST). His research interests include theoretical aspects of computation, VLSI systems, multiplevalued logic, digital signal processing, image sensing, computer vision, biometric authentication, and secure embedded systems. Dr. Aoki received the Outstanding Paper Award at the IEEE International Symposium on Multiple-Valued Logic (ISMVL) in 1990, 2000, 2001 and 2006, the Outstanding Transactions Paper Award from the IEICE of Japan in 1989 and 1997, the IEE Ambrose Fleming Premium Award in 1994, the IEICE Inose Award in 1997, the IEE Mountbatten Premium Award in 1999, the Best Paper Award at the IEEE International Symposium on Intelligent Signal Processing and Communication Systems (ISPACS) in 1999, and the Best Paper Award at the Workshop on Synthesis And System Integration of Mixed Information technologies (SASIMI) in 2007.

Hiroshi Nakajima received the B.E. degree in electronic engineering from Tohoku University, Sendai, Japan, in 1990. He is currently an assistant manager of Development Department 2, Building Systems Company, Yamatake Corporation, Fujisawa, Japan. His research interests include biometric image processing, three-dimensional sensing and processing.

Koji Kobayashi received the B.E. and M.E. degrees in electronic engineering from Tohoku University, Sendai, Japan, in 1976, and 1978, respectively. He is currently a director of Residential Building Department, Building Systems Company, Yamatake Corporation, Tokyo, Japan. His research interests include real-time automation system architecture, network communication protocol LSI, biometric image processing, CMOS image sensor, and three-dimensional sensing.

Tatsuo Higuchi received the B.E., M.E., and D.E. degrees in electronic engineering from Tohoku University, Sendai, Japan, in 1962, 1964, and 1969, respectively. He is currently a Professor at Tohoku Institute of Technology and a Emeritus Professor at Tohoku University. From 1980 to 1993, he was a Professor in the Department of Electronic Engineering at Tohoku University. He was a Professor from 1994 to 2003, and was Dean from 1994 to 1998 in the Graduate School of Information Sciences at Tohoku University. His general research interests include the design of 1-D and multi-D digital filters, linear time-varying system theory, fractals and chaos in digital signal processing, VLSI computing structures for signal and image processing, multiple-valued ICs, multiwave opto-electronic ICs, and biomolecular computing. Dr. Higuchi received the Outstanding Paper Awards at the 1985, 1986, 1988, 1990, 2000, 2001 and 2006 IEEE International Symposiums on Multiple-Valued Logic, the Certificate of Appreciation in 2003 and the Long Service Award in 2004 on Multiple Valued Logic, the Outstanding Transactions Paper Award from the Society of Instrument and Control Engineers (SICE) of Japan in 1984, the Technically Excellent Award from SICE in 1986, and the Outstanding Book Award from SICE in 1996, the Outstanding Transactions Paper Award from the Institute of Electronics, Information and Communication Engineers (IEICE) of Japan in 1990 and 1997, the Inose Award from IEICE in 1997, the Technically Excellent Award from the Robotics Society of Japan in 1990, the IEE Ambrose Fleming Premium Award in 1994, the Outstanding Book Award from the Japanese Society for Engineering Education in 1997, the Award for Persons of scientific and technological merits (Commendation by the minister of state for Science and Technology), the IEE Mountbatten Premium Award in 1999, the Best Paper Award at the 1999 IEEE International Symposium on Intelligent Signal Processing and Communication Systems and the Best Paper Award at the Workshop on Synthesis And System Integration of Mixed Information technologies (SASIMI) in 2007. He also received the IEEE Third Millennium Medal in 2000. He received the fellow grade from IEEE, and SICE.